Novel Bifunctional Periodic Mesoporous Organosilicas, BPMOs: Synthesis, Characterization, Properties and in-Situ Selective Hydroboration−Alcoholysis Reactions of Functional Groups

Tewodros Asefa,[†] Michal Kruk,[‡] Mark J. MacLachlan,[†] Neil Coombs,[†] Hiltrud Grondey,[†] Mietek Jaroniec,[‡] and Geoffrey A. Ozin*,[†]

Contribution from the Materials Chemistry Research Group, Department of Chemistry, University of Toronto, 80 St. George Street, Toronto, Ontario, M5S 3H6, Canada, and Department of Chemistry, Kent State University, Kent, Ohio 44240

Received October 20, 2000. Revised Manuscript Received June 25, 2001

Abstract: A new class of bifunctional periodic mesoporous organosilicas (BPMOs) containing two differently bonded organic moieties in a mesoporous host has been synthesized and characterized. By incorporating bridge-bonded ethylene groups into the walls and terminally bonded vinyl groups protruding into the channel space, both the chemistry and physical properties of the resulting BPMO could be modified. The materials have periodic mesoporous structures in which the bridging ethylene plays a structural and mechanical role and the vinyl groups are readily accessible for chemical transformations. The vinyl groups in the material underwent hydroboration with BH_3·THF and the resulting organoborane in the BPMO was quantitatively transformed into an alcohol using either H_2O_2/NaOH or $NaBO_3$·$4H_2O$. The materials retained ordered structures after subsequent in situ reactions with largely unchanged pore volumes, specific surface areas and pore size distributions. Other organic functionalized BPMO materials may be synthesized in a similar manner or by further functionalizing the resulting borylated or alcohol functionalized BPMO materials. The thermal properties of the BPMO materials have also been investigated and are compared to those of the periodic mesoporous organosilica (PMO) materials. Noteworthy thermal events concern intrachannel reactions between residual silanols or atmospheric oxygen and organics in BPMOs. They begin around 300 °C and smoothly interconvert bridging ethylene to terminal vinyl groups and terminal vinyl to gaseous ethene and ethane, ultimately producing periodic mesoporous silica at 900 °C that exhibits good structural order and a unit-cell size decreased relative to that of the parent BPMO.

Introduction

In recent years, combining organic and inorganic reagents on multiple-length scales to create functional hybrid materials is receiving a great deal of attention.[1] In this way, new materials with unprecedented properties have been prepared.[2] For instance, organic−inorganic hybrid amorphous xerogels, porous hybrid materials with molecularly integrated organic and inorganic groups but broad pore-size distribution have been synthesized and have found various applications.[3,4]

Surfactant-templated hexagonal symmetry forms of mesoporous materials with inorganic frameworks are inorganic−organic nanocomposites with well-defined mesoscopic honeycomb structures. Surfactant removal generates a periodic, monodisperse porous structure with a large surface area and pore volume, making it an attractive platform for applications such as host−guest inclusion,[5] nanotechnology,[6] chemoselective separation and adsorption,[7] chemical sensing,[8] and catalysis.[9] Since the discovery of mesoporous silica in 1992,[10] a large number of ordered mesoporous materials have emerged, includ-

* To whom correspondence should be addressed. E-mail: gozin@alchemy.chem.utoronto.ca.

[†] University of Toronto.

[‡] Kent State University.

(1) (a) Mann, S. *Nature* **1993**, *365*, 499−505. (b) Gomez-Romero, P. *Adv. Mater*. **2001**, *13*, 163−174. (c) Loy, D. A. *MRS Bull.* **2001**, *26*, 364−365.

(2) Fan, H.; Lu, Y.; Stump, A.; Reed, S. T.; Baer, T.; Schunk, R.; Perez-Luna, V.; López, G. P.; Brinker, C. J. *Nature* **2000**, *405*, 56−60.

(3) (a) Loy, D. A.; Shea, K. J. *Chem. Rev*. **1995**, *95*, 1431−1442. (b) Sharp, K. G. *Adv. Mater*. **1998**, *10*, 1243−1248. (c) Moreau, J. J. E.; Wong Chi Man, M. *Coord. Chem. Rev*. **1998**, *178*−*180*, 1073−1084. (d) Girtu, M. A. *J. Optoelectron. Adv. Mater*. **2001**, *3*, 113−118. (e) Corriu, R. J. P. *Angew. Chem., Int. Ed*. **2000**, *39*, 1376−1398. (f) Oviatt, H. W.; Shea, K. J.; Small, J. H. *Chem. Mater*. **1993**, *5*, 943−950.

(4) (a) Guizard, C.; Lacan, P. *New J. Chem.* **1994**, *18*, 1097−1107. (b) Grate, J. W.; Kaganove, S. N.; Patrash, S. J.; Craig, R.; Bliss, M. *Chem. Mater*. **1997**, *9*, 1201−1207. (c) Hernandez, R.; Franville, A.-C.; Minoofar, P.; Dunn, B.; Zink, J. I. *J. Am. Chem. Soc.* **2001**, *123*, 1248−1249.

(5) (a) Ozin, G. A.; Chomski, E.; Khushalani, D.; MacLachlan, M. J. *Curr. Opin. Colloid Interface Sci.* **1998**, *3*, 181−193. (b) Moller, K.; Bein, T.; Fischer, R. X. *Chem. Mater*. **1998**, *10*, 1841−1852. (c) Wu, J.; Gross, A. F.; Tolbert, S. H. *J. Phys. Chem. B* **1999**, *103*, 2374−2384.

(6) (a) Vartuli, J. C.; Shih, S. S.; Kresge, C. T.; Beck, J. S. *Stud. Surf. Sci. Catal.* **1998**, *117*, 13-21. (b) Wang, L. Z.; Shi, J. L.; Yu, J.; Yan, D. S. *J. Inorg. Mater.* **1999**, *14*, 333−342.

(7) (a) Hata, H.; Saeki, S.; Kimura, T.; Sugahara, Y.; Kuroda, K. *Chem. Mater*. **1999**, *11*, 1110−1119. (b) Kemner, K. M.; Feng, X.; Liu, J.; Fryxell, G. E.; Wang, L. Q.; Kim, A. Y.; Gong, M.; Mattigod, S. *J. Synchrotron Radiat.* **1999**, *6*, 633−635. (c) Zhao, D. Y.; Yang, P. D.; Huo, Q. S.; Chmelka, B. F.; Stucky, G. D. *Curr. Opin. Solid State Mater. Sci.* **1998**, *3*, 111−121.

(8) Keefe, M. H.; Slone, R. V.; Hupp, J. T.; Czaplewski, K. F.; Snurr, R. Q.; Stern, C. L. *Langmuir* **2000**, *16*, 3964−3970.

(9) (a) Pater, J. P. G.; Jacobs, P. A.; Martens, J. A. *J. Catal.* **1999**, *184*, 262−267. (b) Morey, M. S.; Davidson, A.; Stucky, G. D. *J. Porous Mater.* **1998**, *5*, 195−204.

(10) (a) Kresge, C. T.; Leonowicz, M. E.; Roth, W. J.; Vartuli, J. C.; Beck, J. S. *Nature* **1992**, *359*, 710−712. (b) Beck, J. S.; Vartuli, J. C.; Roth, W. J.; Leonowicz, M. E.; Kresge, C. T.; Schmitt, K. D.; Chu, C. T−W.; Olson, D. H.; Sheppard, E. W.; McCullen, S. B.; Higgins, J. B.; Schlenker, J. L. *J. Am. Chem. Soc.* **1992**, *114*, 10834−10843.

10.1021/ja0037320 CCC: $20.00 © 2001 American Chemical Society
Published on Web 08/14/2001

ing mesoporous metal oxides,[11] sulfides,[12] and metals.[13] Furthermore, mesoporous materials having terminally bonded organic groups in the channels have been synthesized by addition of $RSi(OR)_3$ precursors during the direct synthesis or postsynthesis.[10b,14−15] These hybrid inorganic−organic materials with reactive organic moieties located in the void space of the material offer opportunities for additional modification via reaction of the organic group, but many of them suffer from the occupation of channel space and inhomogeneities associated with the preparation. More recently, novel periodic mesoporous organosilica (PMO) materials having a uniform distribution of functional organic bridging groups as an integral component of the framework have been reported.[16−21] This approach to functional mesostructures, prepared from the condensation of bis(trialkoxysilyl)organics, $(R'O)_3SiRSi(OR')_3$ (R = ethane, ethylene, methylene, ferrocene, 1,4-phenylene, thiophene, acetylene, etc.), has several advantages over the use of $RSi(OR')_3$ groups: it leaves the void space unoccupied, it may allow the physical properties (e.g., density, refractive index, hardness, fracture toughness) of the framework to be tailored, and it permits chemical modification of the framework by transformation of the bridging organic group. These materials, which incorporate functional organic groups into the framework, have many potential applications.[22,23] Brinker and co-workers have demonstrated the potential for tunable hybrid mesostructures, showing that the dielectric constant and mechanical properties are improved by incorporating bridging organic groups.[24] The combination of increased hardness and decreased dielectric constant may instigate their use in future electronics, optoelectronics, and photonics as functional components of devices and packaging materials.

Mesoporous silica with terminal organic groups have been functionalized to form new mesostructures.[25−28] For instance, the transformation of terminal alkane thiol into sulfonate groups was reported recently.[25] Stein et al. reported the bromination of terminal vinyl groups inside MCM-41 and showed by a kinetic analysis that the organic groups were *inside* the channels.[26] Anwander and co-workers[27] utilized vinyl functionalized disilazane reagents to graft vinyl groups to the silica channel walls of preformed mesoporous silica (MCM-41), which was subsequently hydroborated. We have also demonstrated recently that terminal vinyl groups incorporated directly into mesoporous silica by co-assembling $(EtO)_4Si$ and $(EtO)_3SiCH{=}CH_2$ reagents with surfactant template and base catalyst can be hydroborated and subsequently converted into alcohol groups.[28]

So far, investigations of the PMOs indicate that functional organic groups in the framework are accessible for reaction, but appear to be less reactive than terminal groups due to steric and electronic differences.[16,18] We were inspired to incorporate reactive terminal functional groups into a PMO, a material whose framework chemistry and physical properties could be modulated by the nature and proportion of the organic in the material. In this way, one might form a bifunctional mesostructured material and also learn about the relative reactivities of bridging and terminal organic groups as well as the surface adsorption and physical properties of the materials.

Here we report the first examples of inorganic−organic hybrid bifunctional periodic mesoporous organosilicas (BPMOs) containing both bridging organic functional moieties in the framework and terminal organic functional groups protruding into the channel pores (denoted Class V multifunctional hybrid materials, whose possibility of synthesis was first mentioned in ref 23a). Terminal vinyl groups in the channels can be selectively transformed into alcohols via hydroboration, leaving the bridging ethylene groups intact and retaining ordered mesostructure.

BPMOs are novel materials and are different from PMOs because they contain organic functional groups protruding into the pore void space in addition to organic groups in the channel walls. The organic groups in the framework and in the channels can display different behavior and offer different chemical and physical properties and function to the materials simultaneously. This is partly due to the different environments that they occupy and partly due to the types of organic groups introduced. In particular, the tunability and reactivity of the organic groups inside the pores seems to be higher than those inside the walls. However, the organic groups in the framework give unprecedented physical, mechanical, and hydrophobic−hydrophilic properties to the materials. This enables synthesis of multifunctionally tunable materials whose chemical and physical properties can be tuned simultaneously. This is a property impossible

(11) (a) Antonelli, D. M.; Ying, J. Y. *Angew. Chem., Int. Ed. Engl.* **1996**, *35*, 426−430. (b) Tian, Z.-R.; Tong, W.; Wang, J.-Y.; Duan, N.-G.; Krishnan, V. V.; Suib, S. L. *Science* **1997**, *276*, 926−930.

(12) (a) Braun, P. V.; Osenar, P.; Stupp, S. I. *Nature* **1996**, *380*, 325−328. (b) MacLachlan, M. J.; Coombs, N.; Ozin, G. A. *Nature* **1999**, *397*, 681−684. (c) Rangan, K. K.; Billinge, S. J. L.; Petkov, V.; Heising, J.; Kanatzidis, M. G. *Chem. Mater.* **1999**, *11*, 2629−2632. (d) MacLachlan, M. J.; Coombs, N.; Bedard, R. L.; White, S.; Thompson, L. K.; Ozin, G. A. *J. Am. Chem. Soc.* **1999**, *121*, 12005−12017.

(13) Attard, G. S.; Göltner, C. G.; Corker, J. M.; Henke, S.; Templer, R. H. *Angew. Chem., Int. Ed. Engl.* **1997**, *36*, 1315−1317.

(14) (a) Fowler, C. E.; Burkett, S. L.; Mann, S. *Chem. Commun*. **1997**, 1769−1770. (b) Maquarrie, D. J. *Chem. Commun*. **1996**, 1961−1962. (c) Koya, M.; Nakajima, H. *Stud. Surf. Sci. Catal.* **1998**, *117*, 243−248. (d) Lim, M. H.; Blanford, C. F.; Stein, A. *Chem. Mater*. **1998**, *10*, 467−470. (e) Mercier, L.; Pinnavaia, T. J. *Chem. Mater*. **2000**, *12*, 188−196. (f) Lebeau, B.; Fowler, C. E.; Hall, S. R.; Mann, S. *J. Mater. Chem.* **1999**, *9*, 2279−2281.

(15) (a) Jaroniec, C. P.; Kruk, M.; Jaroniec, M.; Sayari, A. *J. Phys. Chem. B* **1998**, *102*, 5503−5510. (b) Antochshuk, V.; Jaroniec, M. *Chem. Commun.* **1999**, 2373−2374. (c) Jaenicke, S.; Chuah, G. K.; Lin, X. H.; Hu, X. C. *Microporous Mesoporous Mater.* **2000**, *35*−*6*, 143−153. (d) Bhaumik, A.; Tatsumi, T. *Catal. Lett.* **2000**, *66*, 181−184.

(16) Asefa, T.; MacLachlan, M. J.; Coombs, N.; Ozin, G. A. *Nature* **1999**, *402*, 867−871.

(17) Inagaki, S.; Guan, S.; Fukushima, Y.; Ohsuna, T.; Terasaki, O. *J. Am. Chem. Soc*. **1999**, *121*, 9611−9614.

(18) Melde, B. J.; Holland, B. T.; Blanford, C. F.; Stein, A. *Chem. Mater.* **1999**, *11*, 3302−3308.

(19) Yoshina-Ishii, C.; Asefa, T.; Coombs, N.; MacLachlan, M. J.; Ozin, G. A. *Chem. Commun.* **1999**, 2539−2540.

(20) Asefa, T.; MacLachlan, M. J.; Grondey, H.; Coombs, N.; Ozin, G. A. *Angew. Chem., Int. Ed.* **2000**, *39*, 1808−1811.

(21) (a) Guan, S.; Inagaki, S.; Ohsuna, T.; Terasaki, O. *J. Am. Chem. Soc.* **2000**, *122*, 5660−5661. (b) Sayari A.; Hamoudi, S.; Yang, Y.; Moudrakovski, I. L.; Ripmeester, J. R. *Chem. Mater*. **2000**, *12*, 3857−3863. (c) Kruk, M.; Jaroniec, M.; S. Guan, S. Inagaki *J. Phys. Chem. B* **2001**, *105*, 681−689.

(22) MacLachlan, M. J.; Asefa, T.; Ozin, G. A. *Chem. Eur. J*. **2000**, *6*, 2507−2511.

(23) (a) Asefa, T.; Yoshina-Ishii, C.; MacLachlan, M. J.; Ozin, G. A. *J. Mater. Chem.* **2000**, *10*, 1751−1755. (b) Asefa, T.; Coombs, N.; Dag, Ö.; Grondey, H.; MacLachlan, M. J.; Ozin, G. A.; Yoshina-Ishii, C. *Mater. Res. Soc. Proc.* **2000**, *628*, CC3.9.1−CC3.9.8. (c) Dag, Ö.; Yoshina-Ishii, C.; Asefa, T.; MacLachlan, M. J.; Grondey, H.; Ozin, G. A.; *Adv. Funct. Mater*. **2001**, *3*, 213-217.

(24) Lu, Y.; Fan, H.; Doke, N.; Loy, D. A.; Assink, R. A.; LaVan, D. A.; Brinker, C. J. *J. Am. Chem. Soc.* **2000**, *122*, 5258−5261.

(25) (a) Lim, M. H.; Blanford, C. F.; Stein, A. *Chem. Mater*. **1998**, *10*, 467−470. (b) Margolese, D.; Melero, J. A.; Christiansen, S. C.; Chmelka, B. F.; Stucky, G. D. *Chem. Mater.* **2000**, *12*, 2448−2459. (c) Van Rhijn, W. M.; De Vos, D. E.; Sels, B. F.; Bossaert, W. D.; Jacobs, P. A. *Chem. Commun.* **1998**, 317−318.

(26) Lim, M. H.; Blanford, C. F.; Stein, A. *J. Am. Chem. Soc.* **1997**, *119*, 4090−4091.

(27) (a) Anwander, R.; Palm, C.; Stelzer, J.; Groeger, O.; Engelhardt, G. *Stud. Surf. Sci. Catal.* **1998**, *117*, 135−142. (b) Anwander, R.; Nagl, I.; Widenmeyer, M.; Engelhardt, G.; Groeger, O.; Palm, C.; Röser, T. *J. Phys. Chem. B.* **2000**, *104*, 3532−3544.

(28) Asefa, T.; Kruk, M.; MacLachlan, M. J.; Coombs, N.; Grondey, H.; Jaroniec, M.; Ozin, G. A. *Adv. Funct. Mater.* Submitted.

Scheme 1[a]

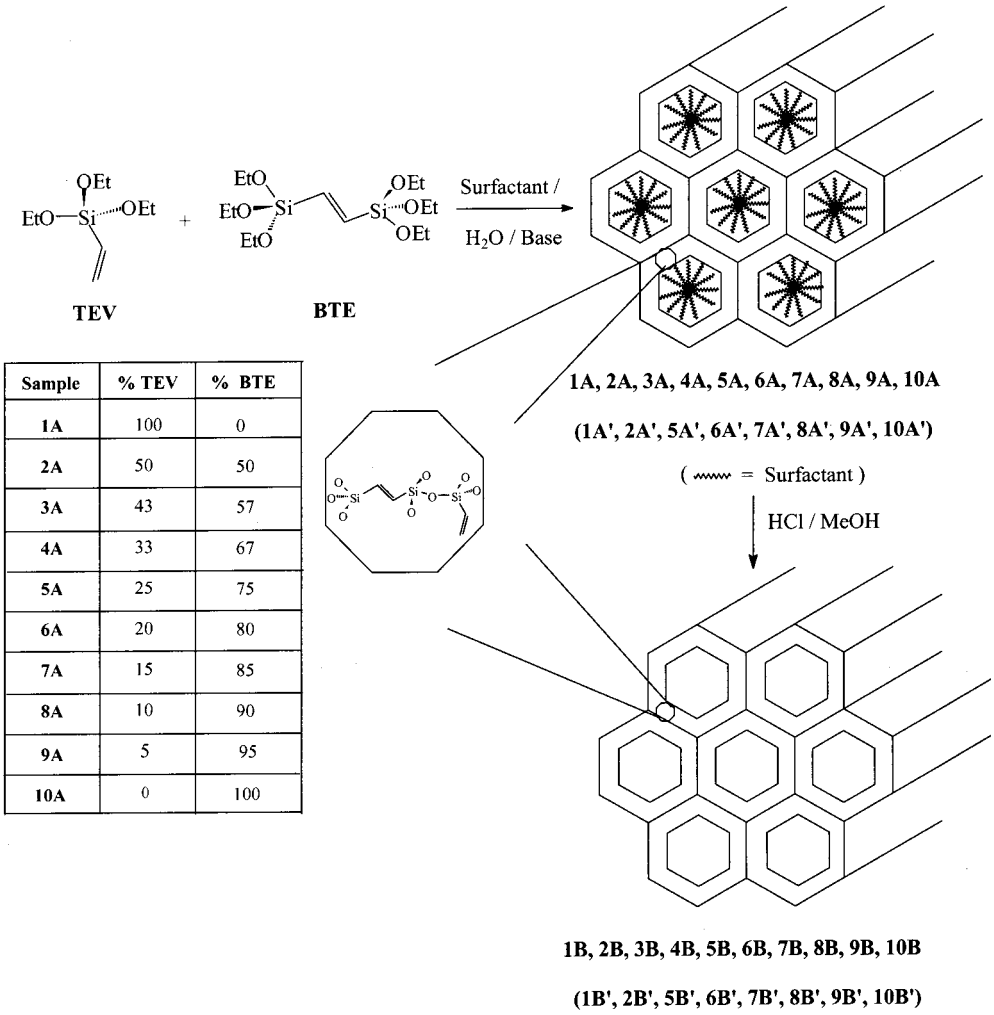

Sample	% TEV	% BTE
1A	100	0
2A	50	50
3A	43	57
4A	33	67
5A	25	75
6A	20	80
7A	15	85
8A	10	90
9A	5	95
10A	0	100

[a] Samples **1A**, **1A′**, **1B**, and **1B′** are amorphous, and the schematic does not represent their structures.

to achieve both in PMOs and terminal organic group functionalized materials**.** For instance, organic groups with various types of properties can be introduced in the same material and in various relative proportions, and if desired, some of these groups can be selectively transformed to obtain materials with the required multifunctionality and tunable properties. The approach we employed for making BPMOs uses direct synthesis and provides an opportunity to achieve a uniform distribution of two or more different kinds of organic functional groups both in the channel walls and inside the pores of ordered mesostructures.

Experimental Section

Materials. Bis(triethoxysilyl)ethylene (BTE) was obtained from Gelest; triethoxyvinylsilane (TEV), borane tetrahydrofuran (BH_3·THF), hydrogen peroxide (H_2O_2, 30 wt %), and all other reagents and solvents were obtained from Aldrich. THF was dried over CaH_2 and distilled from Na/benzophenone before use.

Synthesis of BPMOs. Bifunctional mesoporous materials were prepared using BTE as the source of the bridging organic group and TEV as the source of the terminal organic group. For a typical synthesis, a molar ratio of 1.00 Si:0.26 CTABr:95.07 H_2O:15.73 NH_4OH was used. Samples were prepared with different BTE:TEV ratios (**1A**−**10A**, Scheme 1) using the same procedure, demonstrated for sample **4A**. Another series of samples **1A′**, **2A′**, **5A′**−**10A′** were prepared using a similar procedure and composition of the synthesis mixture, except for the Si:CTAB ratio of 1.00:0.51. Sample **4A** (20% TEV; throughout the manuscript, % TEV indicates the percentage of this precursor expressed per mole of silicon atoms in the BTE and TEV organosilica precursors) was prepared as follows: A solution of cetyltrimethylammonium bromide (CTABr) (1.38 g, 3.79 mmol), ammonium hydroxide (13.23 g, 30 wt %, 0.23 mol), and water (25.05 g, 1.39 mol) was prepared at room temperature. To this solution was added a mixture of BTE (2.06 g, 5.84 mmol) and TEV (0.56 g, 2.94 mmol). The mixture was stirred for 30 min, during which time a white precipitate formed. The materials were aged at 80 °C for 4 days to increase the degree of condensation and enhance the rigidity of the materials (sample **1A** remained a gel even after 1 day of aging, and therefore afterward it was kept in an open plastic bottle in the oven to let the solvent evaporate and obtain a powder). Then the product was filtered, washed with copious amounts of water, and dried under ambient conditions. A fine white powder was obtained (0.9−1.2 g).

Surfactant Extraction. The surfactant was extracted from the samples using an HCl/methanol solution. Typically ca. 0.5 g of as-synthesized powder (**1A**−**10A**) was stirred for 8 h at 55 °C in a solution of 5 g of concentrated (36 wt %) HCl and 150 g of methanol. The product (**1B**−**10B** or **1B′**−**10B′**) was then isolated on a Büchner funnel, washed with methanol, and dried in air. A weight loss of ca. 20−30% was obtained for each sample after a single solvent extraction.

Hydroboration Reactions. Under nitrogen, a suspension of 1.72 g of surfactant-extracted BPMO material **5B** (or **5B′**) in 200 mL of dry THF was cooled to 0 °C. Over 10 min, 35 mL of 1 M borane tetrahydrofuran solution (BH_3·THF) was added to the BPMO suspension. The mixture was stirred for 30 min at 0 °C and then for 6 h at room temperature. Half of the reaction mixture was then quenched by adding ca. 20 mL of water, the other half was quenched with methanol,

and stirring continued for 30 min. The products **5C−I** (or **5C−I′**, from sample **5B′**) and **5C−II** (or **5C−II′**), respectively, were isolated on a Büchner funnel, washed with water or methanol, and dried under air. After being quenched, the hydroborated materials (**5C-I** and **5C−II** or **5C−I′** and **5C−II′**) are air- and moisture-stable for several months.

Alcohol Formation. The hydroborated BPMO was reacted with aqueous $NaOH/H_2O_2$ or aqueous $NaBO_3{\cdot}4H_2O$ to make the corresponding alcohol. The Si−C bond cleaved when an extreme excess of the reagents was used. Typically, for an optimum synthesis ca. 0.4 g of hydroborated BPMO (**5C−I** or **5C−II**) was treated for 12 h with a solution containing either 0.1 g of 0.1 M NaOH and 4 g (30 wt %) of H_2O_2 (or alternatively, 0.4 g of $NaBO_3{\cdot}4H_2O$ in 30 mL of H_2O was used for sample **5C−I′**). The materials were filtered, washed with water, and dried under air. Treatment with dilute HCl regenerated the silanol OH groups.

Instrumentation and Procedures. PXRD patterns and TEM images were obtained using procedures previously described.[12d,20] For in-situ high-temperature PXRD, the diffraction pattern was measured at every 50 or 100 °C interval while the sample was being heated under nitrogen. In these measurements, due to intrinsic displacement of the sample's surface from the "zero" line, caused by slight movement of the HTK-Stage sample holder, all low-angle reflections of different samples (BPMO, ethylenesilica, and vinylsilica materials) were corrected for comparison purposes against a reference material, MCM-41, synthesized and run under the same conditions (d_{100} = 41.28 Å). These corrected observed differences in measured d spacing (Δd) were considered to be a direct representation of the shrinkage of the structures caused by removal of different organic groups. FT-Raman microscope spectra were obtained on an S.A. LabRam Raman microscope. Raman spectra were collected by manually placing the probe tip near the desired point of the sample on a glass slide.

^{13}C, ^{29}Si, and ^{11}B NMR Spectra. Solid-state ^{13}C (100.6 MHz) and ^{29}Si (79.5 MHz) NMR spectra were acquired on a Bruker DSX 400 spectrometer and ^{11}B (64.2 MHz) Hahn-echo NMR spectra were acquired on a Bruker DSX 200 spectrometer. The following experimental parameters were employed: ^{13}C CP-MAS NMR experiments (6.5 kHz spin rate, 3 s recycle delay, 2 ms contact time, $\pi/2$ pulse width of 4.5−7.0 μs, 3000−5000 scans); ^{29}Si CP-MAS NMR experiments (6.5 kHz spin rate, 3 s recycle delay, 10 ms contact time, $\pi/2$ pulse width of 6.0−7.5 μs, 200−1000 scans); ^{29}Si MAS NMR experiments (6.5 kHz spin rate, 100 s recycle delay, $\pi/6$ pulse width of 2.2 μs, 500−1000 scans); ^{11}B Hahn-echo NMR experiments (6.5 kHz spin rate, 0.5 s recycle delay, 0.154 ms dephasing time (dephasing time = 1/spin rate), 100000−150000 scans). Adamantane (major peak, 38.4 ppm vs TMS), $Si[OSi(CH_3)_3]_4$ (major peak, −9.98 ppm vs TMS) and $NaBH_4$ (−42 ppm vs $BF_3{\cdot}OEt_2$) were used as external references for ^{13}C, ^{29}Si, and ^{11}B NMR spectra, respectively.

Nitrogen Adsorption and Thermogravimetry. Nitrogen adsorption isotherms were measured at −196 °C on a Micromeritics ASAP 2010 volumetric adsorption analyzer. Before the measurements the samples were outgassed at 100 °C for >2 h under vacuum, until a residual pressure of ≤6 μm Hg was reached. The BET specific surface area[29a] was evaluated from data in the relative pressure range from 0.01 to 0.02. It was shown elsewhere that this range is suitable for the specific surface area assessment for silicas with pore sizes on the borderline between the micropore and mesopore ranges;[29b] although in the case of the BPMO materials, whose surfaces are organic-functionalized, some degree of underestimation of the surface area can be expected on the basis of earlier studies.[29c] The total pore volume was estimated from the amount adsorbed at a relative pressure of 0.99.[29a] The pore-size distribution was evaluated using the method based on calibration using MCM-41 silicas[29d] and surface-modified MCM-41 silicas.[29c] Adsorption data analysis has been discussed in more detail elsewhere.[29e]

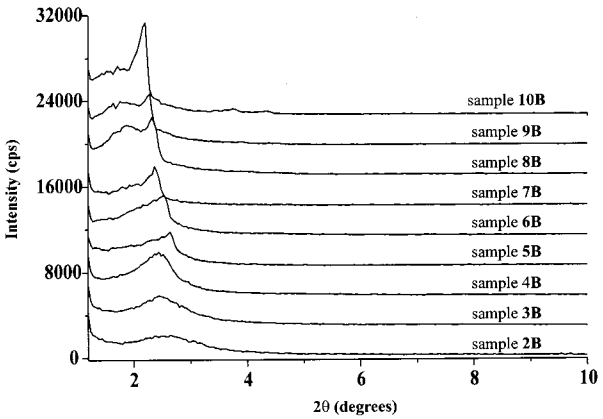

Figure 1. PXRD patterns of **2B−10B** BPMO materials.

Weight change curves were recorded under nitrogen or air atmosphere on a TA Instruments TGA 2950 thermogravimetric analyzer using high-resolution mode with a maximum heating rate of 5 °C min^{-1}.

Results

Synthesis. With the recent interest in developing organized organic−inorganic hybrid materials with potential multiple functions,[30] we identified the periodic mesoporous organosilicas (PMOs) as platform substrates for bifunctional mesoporous materials. By creating structures that incorporated organic groups both in the channels and in the walls, we synthesized materials with new properties. The bifunctional PMOs (BPMOs) were prepared using the supramolecular liquid-crystal templating technique developed at Mobil.[10] In a ca. 4 wt % aqueous surfactant solution containing catalytic base, a mixture of the organosilica precursors was condensed to form a white precipitate. Surfactant was extracted from the as-synthesized materials by treating the BPMOs with warm HCl/methanol. The as-synthesized and surfactant-extracted samples were characterized by powder X-ray diffraction (PXRD), transmission electron microscopy (TEM), N_2 adsorption, thermogravimetric analysis (TGA), Raman spectroscopy, and ^{13}C cross-polarization magic angle spinning (CP-MAS), ^{29}Si CP-MAS, and ^{29}Si MAS NMR spectroscopy.

Powder X-ray Diffraction, TEM, and Porosity. Figure 1A shows the PXRD patterns of nine well-organized surfactant-extracted vinyl-ethylene containing BPMO samples synthesized with 50% or less TEV in the synthesis mixture (**2B−10B**). All of the samples were prepared in a CTABr surfactant-templated system and showed at least one low-angle Bragg peak, indicating the presence of uniformly sized pores in the materials. The PXRD patterns indicate that the intensity of the d_{100} reflection decreases as the TEV:BTE ratio increases. Furthermore, BPMO samples prepared with more than 50% TEV remained amorphous with no observable low-angle PXRD reflections. The amorphous nature of these materials can be related to the fact that the TEV precursor contains fewer hydrolyzable groups (3 in TEV vs 6 in BTE), so that when its amount increases, the degree of cross-linking decreases to such an extent that an ordered mesostructure does not form. A similar trend has been observed in the pure silica analogues, where the incorporation of not more than 40 and 50−60% of organotrialkoxysilane precursor in surface-functionalized organosilicas with uniform pores was reported using ionic and nonionic surfactant templates, respectively.[31] The PXRD patterns (Figure 1A) also indicates a

(29) (a) Sing, K. S. W.; Everett, D. H.; Haul, R. A. W.; Moscou, L.; Pierotti, R. A.; Rouquerol, J.; Siemieniewska, T. *Pure Appl. Chem.* **1985**, *57*, 603−619. (b) Ryoo, R.; Park, I.-S.; Jun, S.; Lee, C. W.; Kruk, M.; Jaroniec, M. *J. Am. Chem. Soc.* **2001**, *123*, 1650−1657. (c) Kruk, M.; Antochshuk, V.; Jaroniec, M.; Sayari, A. *J. Phys. Chem. B* **1999**, *103*, 10670−10678. (d) Kruk, M.; Jaroniec, M., Sayari A., *Langmuir* **1997**, *13*, 6267−6273. (e) Kruk, M.; Jaroniec, M. *Chem. Mater.*, published on Web 5/3/**2001**.

(30) (a) Corma, A.; Kumar, D. *Stud. Surf. Sci. Catal.* **1998**, *117*, 201−222. (b) Corma, A. *Top. Catal.* **1997**, *4*, 249−260. (c) Liu, H. C.; Yang, X. Y.; Ran, G. P.; Min, E. Z. *J. Chem. Res. Synop.* **2000**, 294−295.

d spacing decrease from 40.6 to 33.8 Å from sample **10B** to **2B** as the ratio of terminal organic groups increases, although some irregularity from this trend was observed for higher loadings, as the unit cell size decreased from **10B** to **5B** and then slightly increased for **3B** and **4B**, and decreased for the highest loading (sample 2B). The decrease in the unit-cell size as the loading of pendent organic groups increases has been commonly observed for materials synthesized via co-condensation of TEOS or tetramethyl orthosilicate (TMOS) and organotrialkoxysilane.[31c] Therefore, the decrease in the *d* spacing for BPMOs with increasing the amount of the organotrialkoxysilane (TEV) in the synthesis gel indicates a concomitant increase in the loading of the surface terminally bound organic groups. The procedure of self-assembling BPMO materials also worked well with other surfactants that template the formation of MCM-41. For example, bifunctional samples prepared with cetylpyridinium chloride (CPCl) surfactant also resulted in structurally well-ordered materials (Supporting Information Figure 1A). Similarly, bifunctional BPMO and trifunctional TPMO materials with various other combinations of organic groups (methylene−vinyl, ethylene−methylene−vinyl, etc.) formed well-ordered materials (Supporting Information Figure 1A). Although the number of observable PXRD reflections was not sufficient to unambiguously identify the structure type of the several BPMO materials reported herein, the TEM image of samples **5B** and **5B′** revealed a well-ordered 2-D hexagonal mesostructure (Supporting Information Figure 1B). This structure type is likely to be typical for the other BPMOs under current study, although further TEM studies will be necessary to verify this expectation, especially as PMOs are known to be capable of forming a variety of ordered and disordered structures with observable PXRD reflections and well-defined porosity.[17,18,21]

N_2 adsorption isotherms for the BPMOs exhibited a tendency to change from type IV to I[29a,e] as the amount of TEV in the synthesis gel increased (see Figure 2A and Supporting Information Figure 2). This behavior is typical for materials with gradually decreasing pore diameter on the borderline between mesopore (diameter 20−500 Å) and micropore (diameter below 20 Å) ranges.[29b,e] The BPMOs exhibit size distributions of primary pores[29d] with maxima shifting from about 3.0 to 2.0 nm as the % TEV in the synthesis gel increases from 5 to 50%. The pore diameters provided in Table 1 reflect maxima of pore size distributions (PSDs) calculated using procedures suitable for (i) materials with surface covered by dense layer of hydrocarbon chains[29c] and (ii) materials with siliceous surfaces. The BPMOs under study have surfaces intermediate between these extremes, so that their actual average primary pore size is likely to be between the two values provided in Table 1. The BPMOs under study as well as the ethylenesilica PMO (sample **10B**) exhibit a pronounced secondary porosity, which may be related to their small particle size and to the presence of some disordered domains within the materials. Because the secondary porosity persists for all TEV concentrations in the synthesis gel, the hypothetical development of such disordered domains is not likely to be related to phase separation, that is, the occurrence of separate TEV-rich and BTE-rich domains. The latter phase-separation is also unlikely because the samples with high TEV loadings (100% sample **1B** and 65% sample) were found to be disordered mesoporous materials with broad PSDs centered at about 150 Å (see adsorption data in Supporting Information Figure 2B). No evidence of such porosity was found for BPMOs, suggesting the absence of a TEV-rich phase. The BET specific surface areas for the BPMO samples were in the range from 500 to 700 m^2 g^{-1}, which is slightly lower than the values reported thus far for PMOs.[16−21] The variations of surface area between the samples may be partially caused by the presence of residual surfactant (1−3 wt % as determined from TGA, see below) for the samples with lower surface areas. Moreover, the determination of specific surface area for materials with pore sizes on the borderline between the micropore and mesopore ranges, as well as the comparison of surface areas for materials

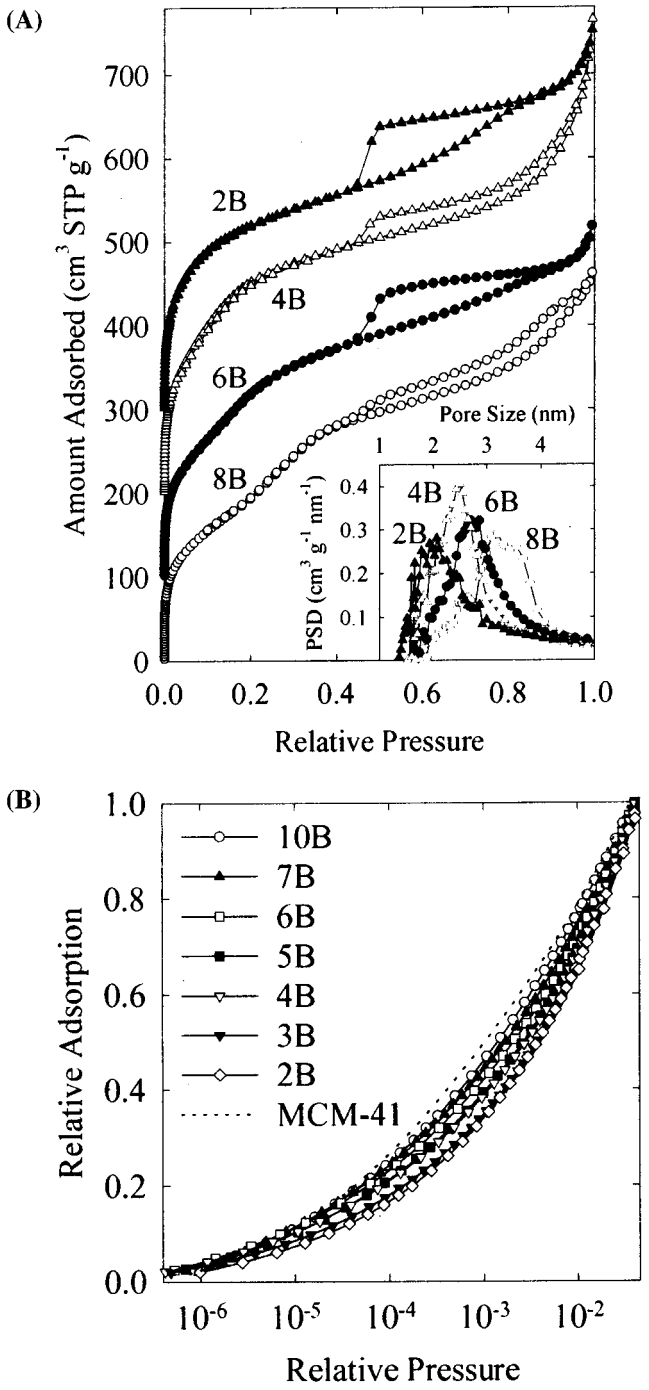

Figure 2. (A) N_2 adsorption isotherms for selected solvent-extracted BPMOs. The isotherms were offset vertically by 100, 200, and 300 cm^3 STP g^{-1} for samples **6B**, **4B** and **2B**, respectively. The corresponding pore size distributions[29d] are shown in the inset. (B) Relative adsorption curves of BPMO samples compared with that of MCM-41 silica.

(31) (a) Burkett, S. L.; Sims, S. D.; Mann, S. *Chem. Commun.* **1996**, 1367−1368. (b) Mori, Y.; Pinnavaia, T. J. *Chem. Mater.* **2001**, *13*, 2173-2178. (c) Stein, A.; Melde, B. J.; Schroden, R. C. *Adv. Mater.* **2000**, *12*, 1403−1419.

Table 1. Structural Properties of BPMOs

sample	BET specific surface area ($m^2\ g^{-1}$)	total pore volume ($cm^3\ g^{-1}$)	pore diameter (Å)
2B	670	0.68	18−21
3B	680	0.76	20−22
4B	650	0.82	22−25
5B	520	0.59	22−25
6B	550	0.62	25−28
7B	610	0.94	29−30
8B	540	0.70	29−31
9B	510	0.64	31−34
10B	500	0.64	34−36

with different surface properties is inherently difficult, as discussed elsewhere.[29e] The total pore volume listed in Table 1 provides the volume of both primary (uniform) and secondary (disordered, perhaps interparticle) pores.

Low-pressure adsorption properties of BPMOs changed systematically as the content of TEV in the synthesis gel increased. As seen from the relative adsorption curves (amounts adsorbed divided by the BET monolayer capacity) (Figure 2B), all the BPMO and PMO samples exhibit weaker low-pressure adsorption than MCM-41 silica (data taken from ref 29b). The difference between MCM-41 and PMO (**10B**) or BPMOs with lower %TEV (**7B**−**9B**; not shown in Figure 2B) was relatively small, as expected from earlier studies of ethanesilica PMO.[21c] However, the BPMOs with higher %TEV in the synthesis mixture exhibited a gradually decreasing low-pressure relative adsorption. Since the introduction of hydrocarbon-based surface groups onto silica surface is known to lower low-pressure relative adsorption,[29e] the behavior observed for the BPMO samples under study strongly suggests an increase in the loading of vinyl groups as the %TEV in the synthesis gel increases.

Spectroscopic Studies. The presence of organic groups in the materials after hydrolysis and condensation was confirmed using solid-state NMR spectroscopy (see Supporting Information Figure 3). The spectra show signals that can be assigned to ethylene at 147 ppm[16,18] and to the vinyl groups at 132 and 136 ppm.[26,32] With increasing proportion of BTE used in the synthesis, the relative intensity of the ethylene carbon peaks with respect to the vinyl carbon peak increases, indicating the incorporation of the organic functional groups into the materials during the synthesis. The organic components of the BPMO materials were also identified in the FT-Raman spectra, Figure 3 (the complete range of spectrum is given in Supporting Information Figure 4). After surfactant extraction, the organic groups remained intact as indicated by the $\nu_{C=C}$ stretching bands of the vinyl and ethylene groups at 1600 and 1570 cm^{-1}, respectively. As the relative amount of TEV used in the synthesis was increased, the intensity of the band assigned to vinyl groups increased compared with that for the ethylene groups. Moreover, a weak band at 1410 cm^{-1}, assigned to the in-plane δ_{C-H} deformation of the CH═*CH*$_2$ groups of the terminal vinyl groups was observed clearly for samples with higher vinyl group loadings. The bands at 1444 and 1300 cm^{-1} are assigned to the in-plane δ_{C-H} deformation of cis and trans bridging ethylene groups, respectively, and increase in intensity as the relative quantity of ethylene groups increases (the starting BTE precursor has ca. 80% trans and 20% cis). The in-plane δ_{C-H} deformation of vinyl groups (*CH*═CH$_2$) was observed at 1275 cm^{-1}, and its intensity decreases and eventually disappears on passing from **5B′** to **10B′**. These results are consistent with the incorporation of terminal vinyl and bridging ethylene groups into the BPMO corresponding to the starting synthesis ratios.

(32) Igarashi, N.; Tanaka, Y.; Nakata, S.; Tatsumi, T. *Chem. Lett.* **1999**, 1−2.

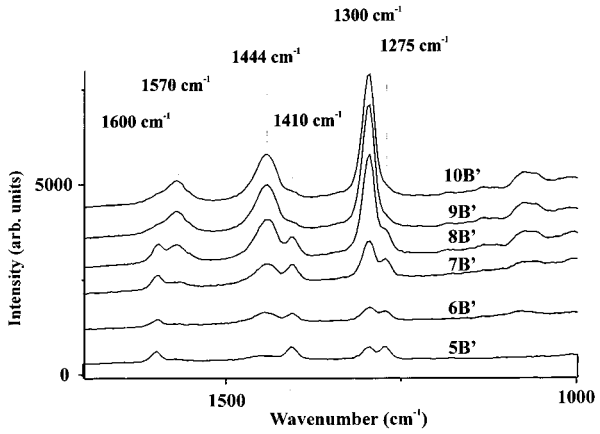

Figure 3. FT-micro-Raman spectra of surfactant-extracted BPMO samples **5B′**−**10B′**.

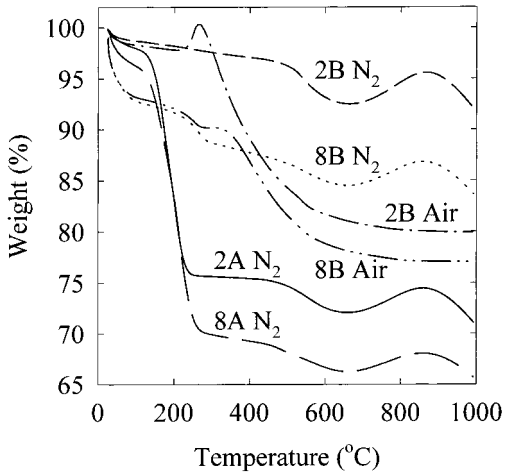

Figure 4. Weight change curves under nitrogen and air of as-synthesized and solvent-extracted BPMO samples **2A**, **8A**, **2B**, and **8B**.

The ^{29}Si MAS and CP-MAS NMR spectrum for representative solvent-extracted samples (presented in Supporting Information Figure 5, A and B, respectively) show the presence of T ($RSiO_3$, $\delta = -63$ to -83 ppm) and the absence or very small population of Q (SiO_4, $\delta = -93$ to -110 ppm) sites, indicating that nearly all of the Si−C bonds remain intact after both synthesis and surfactant extraction. Moreover, from the relative intensities of the T peaks, there are mostly T_3 sites (−83 ppm), fewer T_2 sites, and none or small amounts of T_1 sites. Evidently, the BPMO samples exhibit a high degree of framework cross-linking. ^{29}Si CP-MAS and MAS NMR spectra of samples **1B** and **10B**[16] confirmed that the peaks assigned to T sites are in almost the same positions for both Si atoms that are attached to ethylene and vinyl groups (83 and 81 ppm for T_3, respectively). Furthermore, sample **1A** synthesized from 100% TEV is amorphous and showed mainly T_3 sites as complete cross-linking occurred in this materials (Supporting Information Figure 5).

Thermal Properties. The thermogravimetric analysis (TGA) under nitrogen atmosphere for as-synthesized BPMO samples (data for **2A** and **8A** shown in Figure 4) showed a weight loss below 100 °C related to the removal of physisorbed water. A subsequent large weight loss (22−31% for **2A**−**10A**) observed between 100 and 300 °C can be assigned mostly to surfactant decomposition,[21c] and some additional weight loss between about 400 and 600 °C can be attributed mostly to a partial decomposition of organic groups (vinyl and ethylene). Weight

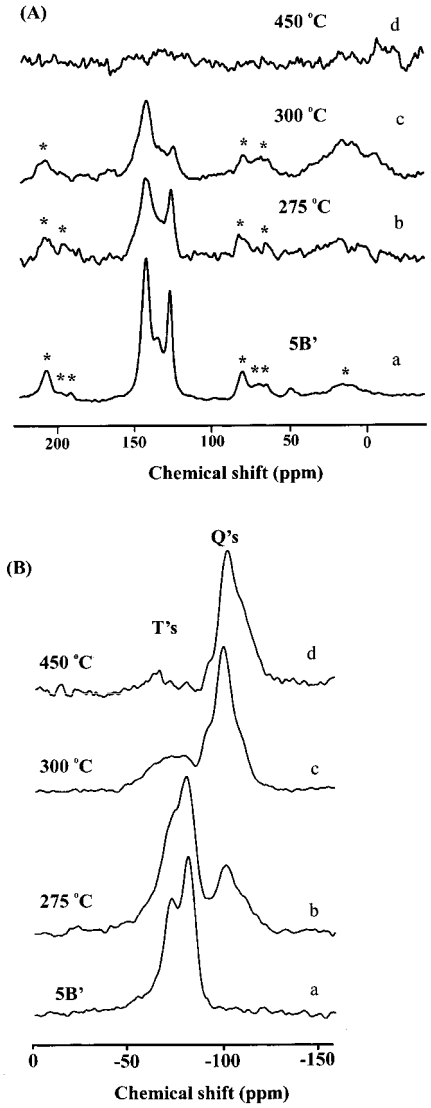

Figure 5. (A) ^{13}C CP-MAS NMR spectra of **5B′** (a) before pyrolysis and after pyrolysis under air for 5 h at (b) 275 °C, (c) 300 °C, and (d) 450 °C (* denotes spinning sidebands). (B) ^{29}Si CP-MAS NMR spectra of **5B′** (a) before pyrolysis and after pyrolysis under air for 5 h at (b) 275 °C, (c) 300 °C, and (d) 450 °C.

gains were observed above 700 °C, most likely because of reaction of partially decomposed bridging organic groups with nitrogen, as already observed for PMOs.[21c] The weight-change patterns for surfactant-extracted materials showed a behavior similar to that of as-synthesized materials below 100 °C and above about 300 °C, but a diminished weight change due to surfactant decomposition (100−300 °C). For some samples, the amount of surfactant indicated by TGA analysis appeared to be negligibly small, if any (0.5 wt % or less for **2B**, **3B**, **4B,** and **7B**); for others, it was 1−3 wt % (see a step at about 250 °C on the weight change curve for **8B** shown in Figure 4), suggesting that in all cases, the degree of surfactant removal was better than 90%. The weight change curves recorded under air for surfactant-extracted materials were somewhat different from those recorded under nitrogen. The initial weight change was similar, including the event of decomposition of the residual surfactant, if any. However, a weight gain was recorded under air at about 300 °C, especially for materials with larger %TEV. This weight gain is most likely related to an oxidation of vinyl groups, which would result in formation of oxygen-containing organic surface species, before they react further and thermodesorb from the surface. At temperatures above 300 °C, a significant weight loss that is largely completed at about 600 °C takes place, which is attributable to the removal of the organics from the material. Indeed, the residue at 1000 °C (mostly SiO_2) and the weight loss attributable to the organic group decomposition correlate well with the BPMO composition expected from the TEV:BTE ratio in the synthesis mixture. This provides an indication of an approximately stoichiometric incorporation of the two organosilica precursors during the BPMO formation. It is also noteworthy that the sample weight at temperatures above 600 °C is much larger under nitrogen than under air. This suggests that an appreciable amount of carbonaceous deposit forms under a nitrogen atmosphere and is not thermodesorbed even at 1000 °C.

To determine the temperature at which the vinyl and ethylene groups decomposed or underwent transformation, ^{13}C and ^{29}Si CP-MAS NMR spectra (Figure 5) of sample **5B′** were measured after calcination at 275, 300, and 450 °C under air. The NMR spectra indicate that the decomposition and transformation of the organic groups in the BPMO begins at ca. 275 °C. Initially, it appears that bridging ethylene groups transform into vinyl groups, and vinyl groups are lost as gaseous ethene. A similar thermal transformation was observed in methylenesilica PMO, where the bridging organic groups reacted with protons from water or silanol groups to form terminal methyl groups, which were then eliminated.[20] Transformation of vinyl into ethyl groups and into a small percentage of ethanol groups was also observed, these being lost as ethane and ethanol (Scheme 2). Similar results were also observed when a pure vinyl-terminated sample (**1B′**) and a pure ethylene-bridged sample (**10B′**) were treated under similar conditions (see Supporting Information Figure 6 and Scheme 2). Pyrolysis MS of **5B′** showed ethylene as the major and ethanol and ethane as the minor pyrolysis products. Further pyrolysis of the materials leads to the decomposition of all the organic groups, and the annealing of the samples, to an ordered, mesoporous silica. These results are summarized in Scheme 2. The periodic structure of the materials, however, was maintained but with a significant shrinkage in the unit cell size. The evolution of the periodic structure in the BPMO material **5B′** during the pyrolysis was monitored by in-situ high-temperature PXRD under nitrogen (Figure 6). The temperature was increased from room temperature to 900 °C at ca. 10 °C min^{-1}, and the PXRD pattern was measured at every 50 or 100 °C. The position of the 100 peak remained unchanged up to 300 °C before the organic groups started to transfer and decompose. Thereafter, the position of the 100 peak shifted to higher angle (smaller *d* spacing) concomitant with the transformation and decomposition of the organic groups as measured by TGA and NMR. A unit cell contraction (Δa_o) of 13.6 Å (decrease in a_0 from 41.2 to 29.5 Å) was observed after calcination of the BPMO from room temperature to 900 °C under nitrogen (Figure 6B). This contraction probably results from a structural reorganization associated with the replacement of the bridging organosiloxane groups with Si−CH═CH$_2$ and Si−O−Si groups and the condensation of residual silanols. A higher degree of shrinkage begins at ca. 400 °C where major loss and transformation of the organic groups start. The degree of unit-cell size contraction for the BPMO is similar to that for ethylenesilica PMOs (d_{100} decreases by about 12 Å), but higher than for methylenesilica PMOs (about 5 Å) after pyrolysis under similar conditions. The larger shrinkage of the pore size in the bifunctional and ethylenesilica materials compared to the methylenesilica materials upon thermolysis is attributed to the longer organic spacer between Si atoms.

Scheme 2. Thermal Transformation in BMPOs

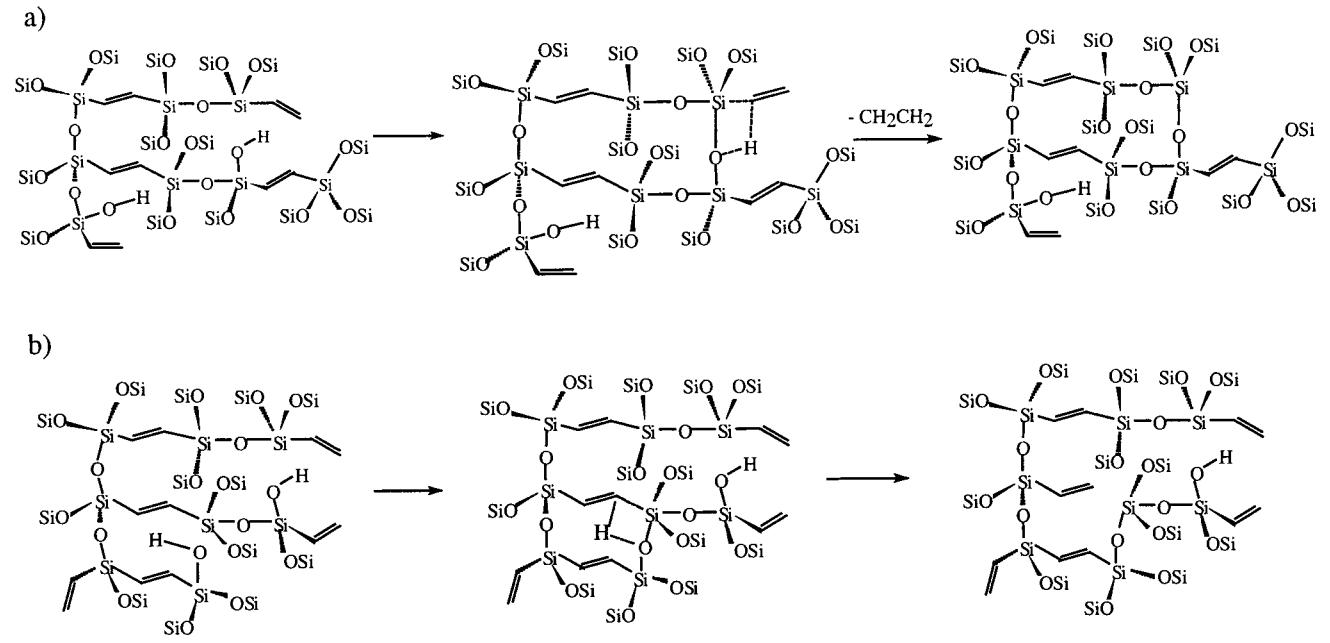

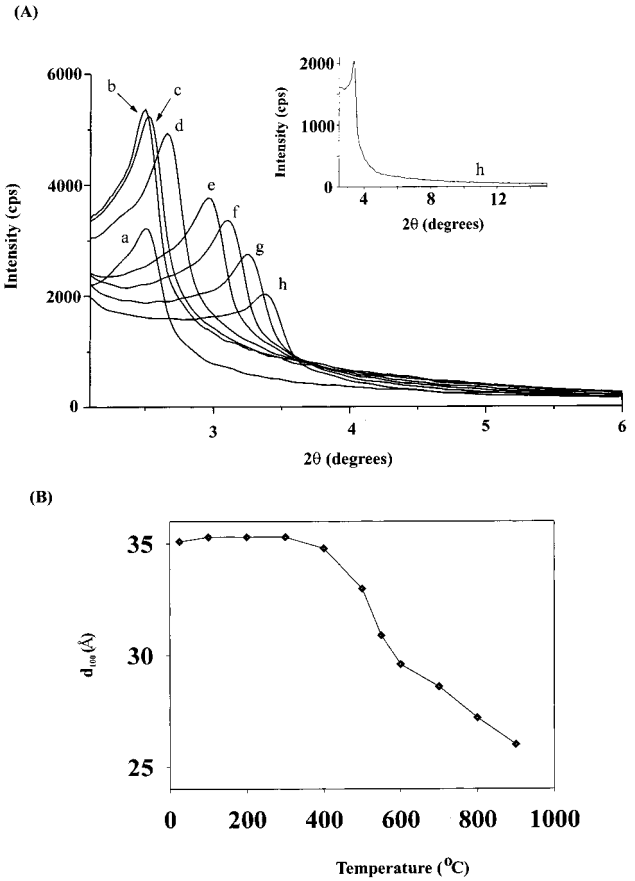

Figure 6. (A) In-situ high-temperature PXRD patterns of **5B′** (under N_2) at (a) room temperature, (b) 200, (c) 300, (d) 400, (e) 600, (f) 700, (g) 800, and (h) 900 °C. (B) The corresponding *d*-spacing for (100) reflection versus temperature plot.

Hydroboration. Discovered and developed by H. C. Brown, hydroboration is routinely used in organic synthesis and has great synthetic utility due to the highly important functional group transformations alkylboranes undergo.[33] Hydroboration of vinyl/ethylene groups in BPMO could therefore be a route to new functional groups in mesoporous materials.

In-situ hydroboration was performed on sample **5B** and **5B′**. Solid-state NMR indicated that the vinyl groups underwent hydroboration while most of the ethylene groups remained unreacted under the synthetic conditions employed (see Experimental Section). To account for reaction with residual silanol groups, a reasonable excess of BH_3·THF was used (Si−C bond cleavage occurs when a large excess of BH_3·THF is used). Figure 7A shows the ^{13}C CP-MAS NMR spectra of sample **5B** after hydroboration and after subsequent oxidation and formation of an alcohol. The peaks initially observed at 132 and 136 ppm (Supporting Information Figure 3) corresponding to vinyl carbons disappeared almost completely and a new broad peak centered at 7 ppm corresponding to sp^3 hybridized carbons emerged (Figure 7A). The resonance corresponding to bridging ethylene carbons at 147 ppm, however, changed very little after the hydroboration reaction. The selective hydroboration of the terminal vinyl groups can be ascribed to the steric and electronic differences between the two organic groups. This interesting selectivity can be taken advantage of to give the BPMOs important bifunctional properties as the bridging organic group maintains the integrity of the structure, which can give unique physical and mechanical properties while the terminal groups undergo the required organic transformations useful for many applications.

These organic group transformations have also been supplemented by the ^{29}Si MAS NMR spectra, presented in Figure 7B (and ^{29}Si CP-MAS spectra in Supplementary Figure 7A). After hydroboration, the position of T sites due to the hydroborated terminal vinyl moiety (Si atom attached to sp^3 carbons) shifted downfield ($T_3 = -67$, $T_2 = -57$ ppm) while the position of the T sites for Si atoms attached to the unreacted bridging ethylene remained unchanged ($T_3 = -83$, $T_2 = -73$ ppm). This trend is consistent with the relative positions of T sites observed for *Si*-C(sp^2) versus *Si*-C(sp^3) silicon atoms.[3e,3f, 28]

The hydroboration of the BPMO materials was also followed by ^{11}B NMR spectroscopy. A Hahn-echo experiment[34] was

(33) Allinger, N. L.; Cava, M. P.; Jongh, D. C. D.; Johnson, C. R.; Lebel, N. A.; Stevens, C. L. *Organic Chemistry;* Worth Pub., Inc.: New York, 1971; p 322.

(34) Hahn, E. L. *Phys. Rev.* **1950**, *80*, 580−585.

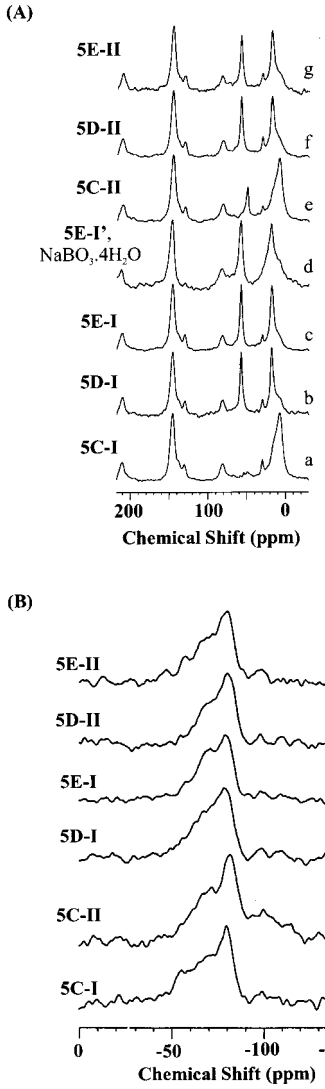

Figure 7. (A) ^{13}C CP-MAS NMR spectra of (a) borylated BPMO, **5C-I**, (b) alcohol BPMO, **5D-I**, (c) alcohol BPMO, **5E-I**, (d) alcohol **5E-I′** treated with mild $NaBO_3$·$4H_2O$ solution, (e) borylated BPMO, **5C-II**, (f) alcohol BPMO, **5D-II**, (g) alcohol BPMO, **5E-II**. (B) ^{29}Si MAS NMR spectra of (a) borylated BPMO, **5C-I**, (b) borylated BPMO, **5C-II**, (c) alcohol BPMO, **5D-I**, (d) alcohol BPMO, **5E-I**, (e) alcohol BPMO, **5D-II**, and (f) alcohol BPMO, **5E-II**.

chosen in order to dephase the ^{11}B background signal stemming from the boron nitride stator in the MAS probe. Figure 8A shows the ^{11}B NMR spectra after hydroboration and methanol quenching of solvent-extracted BPMO (**5B′**), ethylene PMO (**10B′**), and vinylsilica (**1B′**). It also includes spectra for an MCM-41 control after hydroboration and subsequent hydrolysis with dilute HCl. The spectra all show a sharp resonance peak at ca. −1.0 ppm due to hydroboration of residual surface silanols, resulting in Si−O-*B*$(OMe)_2$ groups. The hydroborated silanols could be regenerated by stirring the alcohol functionalized materials in dilute HCl/H_2O solution as revealed by the substantial decrease in the intensity of the sharp peak at ca. −1.0 ppm (Figure 8A). The materials containing unsaturated organic groups (vinyl or ethylene), also showed a broad resonance peak centered at ca. −34 ppm due to hydroborated organic groups in the materials (e.g. Si−CH_2−CH_2−B$(OMe)_2$). Notably, sample **10B′**, which contains only bridging ethylene groups, showed only a trace of hydroboration, affording few Si−CH_2−CH[*B*$(OMe)_2$]−Si groups under the same experimental conditions.

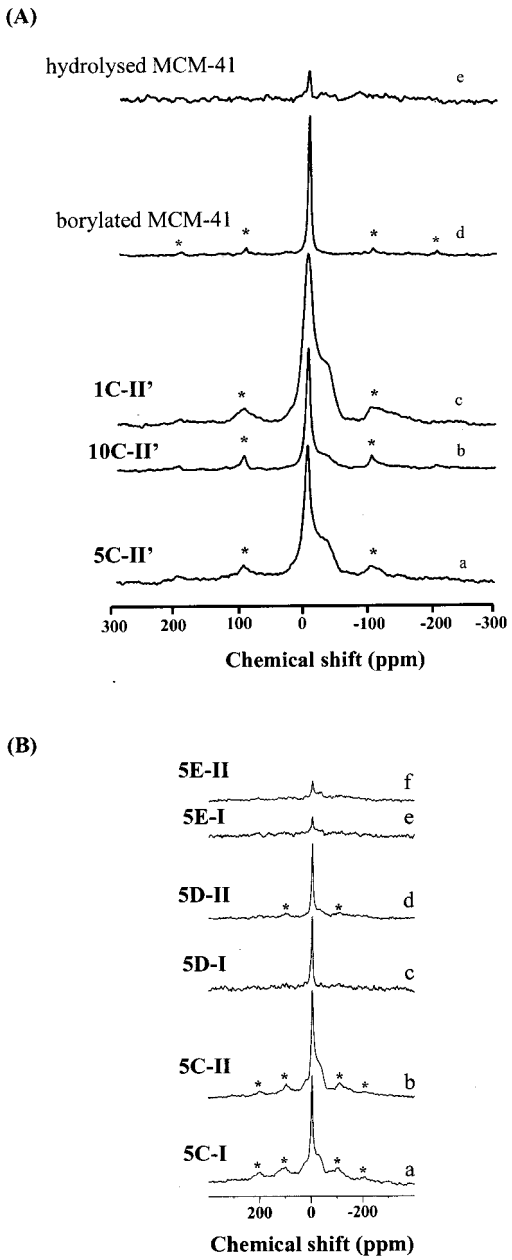

Figure 8. (A) ^{11}B Hahn-echo NMR spectra after hydroboration in BH_3·THF and quenching with methanol of surfactant-extracted (a) **5B′**, (b) **10B′**, (c) **1B′**, (d) mesoporous silica (MCM-41), and (e) after hydrolysis of hydroborated MCM-41 sample in dilute HCl/H_2O solution. (B) ^{11}B Hahn-echo NMR spectra of (a) borylated BPMO, **5C-I**, (b) borylated BPMO, **5C-II**, (c) alcohol BPMO, **5D-I**, (d) alcohol BPMO **5D-II**, (e) alcohol **5E-I**, (f) alcohol BPMO **5E-II**.

The hydroborated material was treated with mild NaOH/H_2O_2 or $NaBO_3$·$4H_2O$ solution to transform the hydroborated alkene into an alcohol. Sodium perborate ($NaBO_3$·$4H_2O$) is an alternative oxidizing agent and has been successfully used to oxidize alkene and alkyne boronic acids and esters in the presence of aldehydes and ketones.[35] ^{13}C CP-MAS NMR confirmed **a** quantitative transformation of the alkylboranes to alcohol groups. After the alcoholysis reaction, the single broad peak observed at 7 ppm in the hydroborated BPMO sample splits into two peaks at ca. 18 and 58 ppm (Figure 7A), corresponding to Si−*C*H_2−CH_2OH and Si−CH_2−*C*H_2OH carbons, respectively. The ^{29}Si MAS NMR spectrum (Figure 7B) shows that the T:Q ratio

(35) Kabalka, G. W.; Yu, S.; Li, N.-S. *Can. J. Chem.* **1998**, *76*, 800−805.

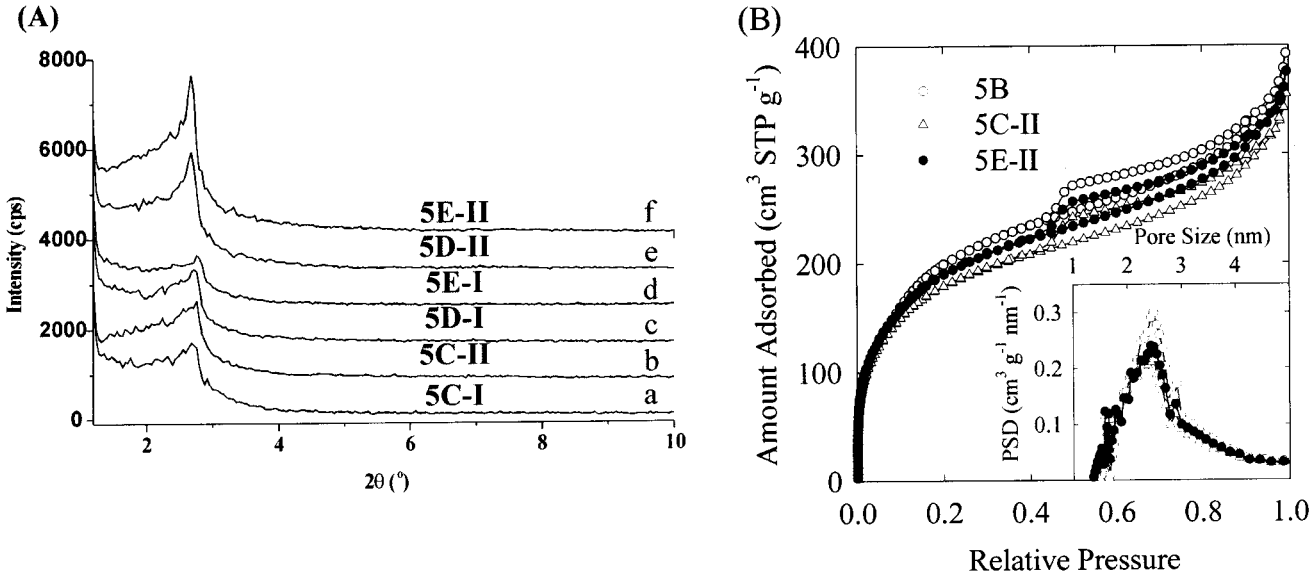

Figure 9. (A) PXRD patterns of (a) borylated BPMO, **5C-I**, (b) borylated BPMO, **5C-II**, (c) alcohol BPMO, **5D-I**, (d) alcohol BPMO, **5E-I**, (e) alcohol BPMO, **5D-II**, and (f) alcohol BPMO, **5E-II**. (B) N_2 adsorption/desorption isotherms of **5B** compared with corresponding selected borylated and alcohol BPMOs. (Inset shows corresponding pore-size distributions[29d]).

Scheme 3. Hydroboration and Oxidation of BPMOs

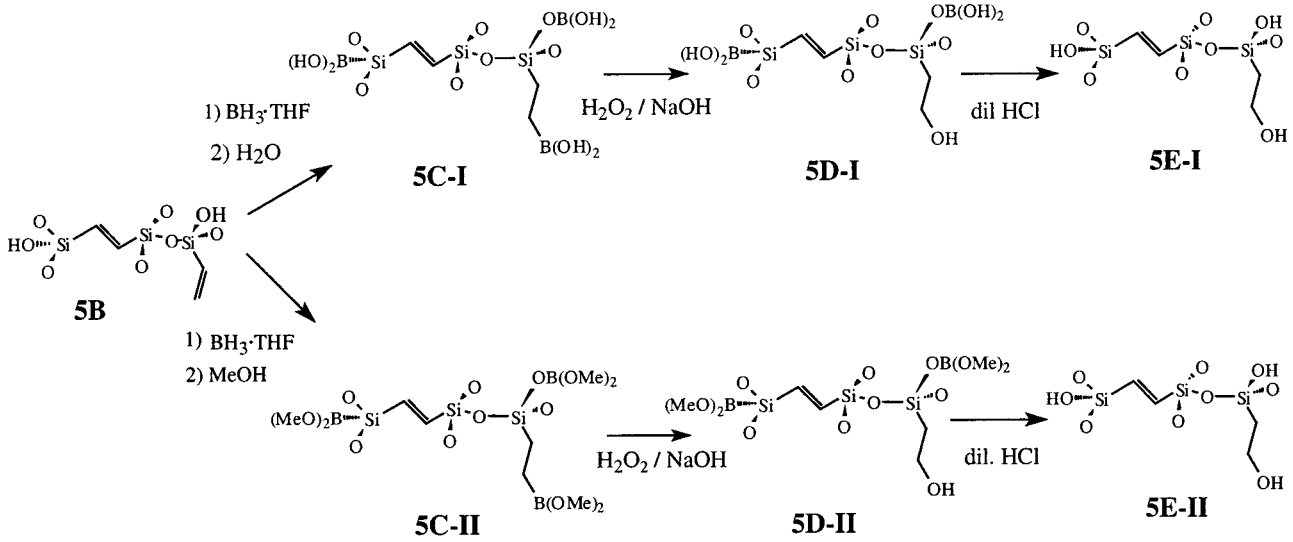

remained unchanged indicating that the Si−C bonds remain intact during the alcoholysis procedure employed (when excess $NaOH/H_2O_2$ or $NaBO_3{\cdot}4H_2O$ was used, a significant cleavage of Si−C bonds were observed). However, the T sites for the Si atoms attached to the ethyl alcohol group were observed upfield from the T sites of Si atoms in the hydroborated samples ($T_3 = -71$ ppm) (these assignments are clearly observable in Supporting Information Figure 7). Scheme 3 depicts the hydroboration and alcoholysis of BPMOs.

Furthermore, as Figure 8B indicates, the broad peak at ca. −30 ppm assigned to $RB(OR')_2$ vanished following oxidation in excess $NaOH/H_2O_2$ or $NaBO_3{\cdot}4H_2O$, indicating complete conversion of hydroborated alkene groups while the hydroborated silanols remained intact. These results are consistent with the results obtained from ^{29}Si (CP) MAS NMR spectroscopy. Further, hydrolysis of the borylated BPMO materials resulted in the significant reduction of peak at ca. −1.0 ppm, which indicated a significant extent of regeneration of the silanol groups.

The conversion of the hydroborated BPMO required careful optimization. When an excess of oxidizing agent was employed, the BPMO samples partially or completely dissolved and their structures collapsed due to cleavage of the framework Si−C bonds. Undissolved samples remaining after partial dissolution showed the presence of some alcohol by NMR, but the periodic mesoporous structure was absent. When stoichiometric or substoichiometric quantities of very dilute $NaOH/H_2O_2$ or $NaBO_3{\cdot}4H_2O$ were employed, the cleavage of the framework Si−C bonds was avoided and no additional Q sites were observed in the ^{29}Si CP-MAS NMR spectra of the samples. It should be noted that oxidative cleavage of Si−C bonds with H_2O_2 is not uncommon.[36]

The periodic mesoporous structure of the material was maintained after the in-situ hydroboration and alcoholysis reactions. Figure 9A shows the PXRD pattern of 5B after

(36) (a) Bittner, S.; Temtsin, G.; Asefa, T.; MacLachlan, M. J.; Ozin, G. A. unpublished results. (b) Jones, G. R.; Landais, Y. *Tetrahedron* **1996**, *52*, 7599−7662.

hydroboration and subsequent transformation into an alcohol. The change in the unit cell dimension of the material after both reactions was insignificant as expected if the organic groups in the framework remain virtually unchanged and only the terminally attached organic groups react. It is also worth noting that the structure of the material was retained after hydroboration and alcoholysis (the shape of the adsorption isotherm did not change, see Figure 9B) and the specific surface areas, pore volumes and PSDs (for the latter, see insets in the Figure) also remain largely unchanged under the optimum conditions employed. This is in contrast with the behavior of vinyl-functionalized MCM-41 synthesized via co-condensation. This material suffered a prominent unit cell shrinkage, pore size decrease, significant loss of the specific surface area and pore volume, as well as decrease in the structural ordering during the alcoholysis step.[28] Apparently, BPMOs are much more stable under basic conditions than organic-functionalized materials with siliceous frameworks synthesized via co-condensation.

Summary and Conclusions

Bifunctional periodic mesoporous materials can be prepared by combining terminal and bridging organic groups into the same material. Although we have focused on the vinyl/ethylene BPMO for the proof-of-concept experiment, the BPMO may be extended to other organics. We have also synthesized well-ordered BPMOs incorporating ethylene/methyl and methylene/vinyl, as well as trifunctional PMOs incorporating ethylene/methylene/vinyl and ethylene/methylene/methyl organic functional moieties. The synthesis can be generalized to create a variety of hybrid materials with organic groups grafted and incorporated into the BPMO.

The vinyl-to-ethanol conversion in the vinyl/ethylene BPMO proceeds with surprising selectivity in 2 steps despite the chemical similarity between the terminal vinyl groups and the bridging ethylene groups in the framework. The difference in reactivity is likely to be attributable to steric factors, but electronic differences associated with the π electrons and polarity of ethylene and vinyl groups may also contribute. The use of bulkier boranes may also enhance the selectivity. After selective transformation of the vinyl group, it may be possible to functionalize the ethylene groups; Ozin et al.[16] and Stein et al.[18] have demonstrated that at least some of the bridging ethylene groups are accessible for bromination in the ethylene-silica PMO and may undergo other transformations as well.

The concept of including two different organic groups into a mesoporous material, where one is terminally attached and one is an integral part of the framework, may lead to the development of bifunctional size-selective catalytic materials with tunable mechanical properties, a great advantage when working with supported catalysts and separation materials. Alternatively, the organic component in the framework may be used to modify the dielectric or optical properties. In a bifunctional material containing a bridging electroactive species and an anchored catalytically active species, for example, it may be possible to electrochemically tune the pore-size and surface charge and thus the catalytic selectivity. The potential for multifunctionalmaterials based on BPMOs is being further explored in our laboratory.

Acknowledgment. This work was supported by the Natural Sciences and Engineering Research Council (NSERC) of Canada. G.A.O. is a Canada Research Chair in Materials Chemistry. M.J.M. thanks NSERC for post-graduate (1995−99) and postdoctoral (1999− 2001; M.I.T.) fellowships. M.J. acknowledges support by NSF Grant CHE-0093707.

Supporting Information Available: PXRD patterns of BPMOs prepared with CPCl surfactant; TEM images of BPMOs, **5B** and **5B′**; N_2 adsorption isotherms of BPMOs, **3B**, **5B**, **7B**, **9B**, and **10B** with corresponding pore size distributions; N_2 adsorption isotherms of 65% and 100% TEV made samples with their pore size distributions; ^{13}C CP MAS NMR spectra of as-synthesized and surfactant-extracted BPMOs; FT-micro-Raman spectra of surfactant-extracted BPMOs; ^{29}Si MAS and CP MAS NMR spectra of surfactant-extracted BPMOs; ^{13}C and ^{29}Si CP MAS NMR spectra of vinylsilica (**1B′**) and ethylenesilica (**10B′**) materials after pyrolysis at 275 and 360 °C for 5 h; ^{29}Si CP MAS NMR spectra of **1B′**, **5B′**, **10B′** and MCM-41 after borylation and alcoholysis (PDF). This material is available free of charge via the Internet at http://pubs.acs.org.

JA0037320